BF-1623
[1-9]

RESEARCH ARTICLE Indian Journal of Animal Research

Metabonomic Method to Analyze the Changes in Pancreatic metabolites in Tree Shrew Traumatic Systemic Inflammatory Response Syndrome After Treatment with Umbilical Cord Mesenchymal Stem Cells

Guang-Ping Ruan[1, 2, 3], Xiang Yao[1, 2, 3], Kai Wang[1, 2, 3], Shu-Qian Lin[1, 2, 3], Rong-Qing Pang[1, 2, 3], Xing-Hua Pan[1, 2, 3]

10.18805/IJAR.BF-1623

ABSTRACT

Background: The impact method was used to make unilateral femoral comminuted fractures in tree shrews, which were then intravenously injected with lipopolysaccharide to create a traumatic systemic inflammatory response syndrome model.

Methods: The treatment group was infused with tree shrew umbilical cord mesenchymal stem cells via the tail vein. After 10 days of treatment, 6 tree shrews were killed in the control, model and treatment groups and pancreatic tissue was collected for metabonomic analysis.

Result: The 25 differential metabolites in the normal, model and stem cell treatment groups showed a trend of first decreasing and then increasing and 11 metabolites showed a trend of first increasing and then decreasing. These findings are in line with the recovery of the curative effect of the stem cell therapy model group.

Key words: Metabolites, Metabolomics, Pancreas, Systemic inflammatory response syndrome, Tree shrew, Umbilical cord mesenchymal stem cells.

List of abbreviations: CV: Coefficient of variation; PLSDA: Partial least squares discriminant analysis; QC: Quality control; SIRS: Systemic inflammatory response syndrome.

INTRODUCTION

Systemic inflammatory response syndrome (SIRS) is a systemic nonspecific inflammatory response to severe injury caused by infectious or noninfectious factors such as infection, trauma, burns, surgery and ischemia-reperfusion and represents a group of clinical symptoms that ultimately lead to the body's uncontrolled inflammatory response. Systemic responses to severe infection include changes in body temperature, respiration, heart rate and white blood cell count [Fang *et al*., 2016;Wagner *et al*., 2016;Anderson and Singh, 2017;Ward *et al*., 2017;Garcia-Lamberechts *et al*., 2018;Li *et al*., 2018; Mahassadi *et al*., 2018;Xu, 2019].

A traumatic systemic inflammatory response syndrome model was established in 30 tree shrews using the impact method to make unilateral femoral comminuted fractures followed by intravenous injection of lipopolysaccharide. Another 10 normal tree shrews were taken as the control group and 10 were given treatment after the model was established (the treatment group) and were infused with tree shrew umbilical cord mesenchymal stem cells via the tail vein. After 10 days of treatment, 6 tree shrews were killed in the control, model and treatment groups and pancreatic tissue was collected for metabolomic analysis.

[1] The Basic Medical Laboratory of 920th Hospital of Joint Logistics Support Force of PLA (Kunming, Yunnan, 650032, China).
[2]The Integrated Engineering Laboratory of Cell Biological Medicine of State and Regions (Kunming, Yunnan, 650032, China).
[3]The Transfer Medicine Key Laboratory of Cell Therapy Technology of Yunan Province (Kunming, Yunnan, 650032, China).

Corresponding Author: Guang-Ping Ruan and Xing-Hua Pan, The Basic Medical Laboratory of 920th Hospital of Joint Logistics Support Force of PLA (Kunming, Yunnan, 650032, China).
Email: ruangp@126.com, xinghuapan@aliyun.com

How to cite this article: Guang-Ping, R., Yao, X., Wang, K., Shu-Qian, L., Rong-Qing, P. and Xing-Hua, P. (2023). Metabonomic Method to Analyze the Changes in Pancreatic metabolites in Tree Shrew Traumatic Systemic Inflammatory Response Syndrome After Treatment with Umbilical Cord Mesenchymal Stem Cells. Indian Journal of Animal Research. doi:10.18805/IJAR.BF-1623

Submitted: 28-12-2022 **Accepted:** 28-03-2023 **Online:** 10-05-2023

MATERIALS AND METHODS

Construction of the tree shrew traumatic systemic inflammatory response syndrome model

Thirty tree shrews were modeled with unilateral femoral comminuted fracture by the heavy object impact method and

then 0.5 mg of lipopolysaccharide was injected intravenously to create a traumatic systemic inflammatory response syndrome model. Another 10 tree shrews were used as the normal control group. The identification of the model can be found in the published literature [Ruan *et al*., 2021].

All experimental protocols were approved by the Experimental Animal Ethics Committee of the 920th Hospital of Joint Logistics Support Force of PLA. All methods were performed in accordance with the relevant guidelines and regulations. The name of the Institute where work were carried out is the 920th Hospital of Joint Logistics Support Force of PLA. The year of experiment (Research period) is in 2020-2021.

Treatment of the tree shrew traumatic systemic inflammatory response syndrome model

Twenty-five of the 30 tree shrew models were successfully constructed and 10 were selected as the treatment group. One hundred microliters of umbilical cord mesenchymal stem cell suspension (1×10^6 cells) was reinfused into the tail vein. The preparation and identification of umbilical cord mesenchymal stem cells were described in published literature [Ruan *et al*., 2016].

Collection of three groups of tree shrew pancreases

After 10 days of treatment, 6 tree shrews each in the control group (Group A), the model group (Group B) and the treatment group (Group C) were killed and the pancreatic tissue was washed with PBS, quickly placed into liquid nitrogen and sent to Hangzhou Lianchuan Biotechnology LC Science for metabolomic assays.

Chromatographic and mass spectrometry conditions

The liquid phase system is an ultrahigh-pressure liquid phase system (SCIEX, UK). The chromatographic column used was an ACQUITY UPLC T3 (100 mm*2.1 mm, 1.8 µm, Waters, UK). During acquisition, the column temperature was set to 35°C and the flow rate was 0.4 ml/ml. The mobile phases used were phase A: water (1% formic acid) and phase B: acetonitrile (1% formic acid). The liquid phase gradient was set in Table 1.

The high-resolution mass spectrometer used for acquisition was a TripleTOF 6600 Plus (SCIEX, UK) time-of-flight mass spectrometer. One positive ion mode acquisition and one negative ion mode acquisition were performed for each sample. The shield air pressure of the ion source was 30 PSI (pounds per square inch) and the gas 1 (auxiliary) and gas 2 (sheath) pressures were both set to 60 PSI. The source temperature was 650 degrees. The voltages were positive 5000 volts in positive ion mode and -4500 volts in negative ion mode. The mode of data acquisition was IDA (information-dependent acquisition) mode.

In one acquisition cycle, the primary acquisition range was 60-1200 Daltons, the primary acquisition time was 150 ms and the primary spectrum was selected based on positive charge (one negative charge in the negative ion mode) and signals per second. The first 12 signal ions with accumulated intensities over 100 were scanned for secondary fragmentation. The entire acquisition cycle took 0.56 seconds.

The mass spectrometer detector has 4 channels, the frequency of the pulsed radio frequency is 11 kHz and the detection frequency of the detector is 40 GHz. The particle signal of each scan was recorded four times in four channels and then combined into data. The dynamic exclusion time for scans was set to 4 seconds.

During acquisition, instrument accuracy corrections were performed at 20-sample intervals. At the same time, QC samples were scanned every 10 samples. The mass gap between QCs was used to correct for systematic errors across the batch.

Use of the metabolomic method to analyze the differences in metabolites in the pancreatic tissues of the three groups of tree shrews

The metabolites in the samples were separated and the corresponding differential metabolites were identified by searching the metabolic database.

Metabolites were extracted from each group of samples. After the extraction of metabolites, an equal amount of extraction solution was drawn from each sample and mixed into QC samples. All samples and QC samples were put on the LC-MS/MS mass spectrometer in turn. Every 10 experimental samples, insert A QC sample mass spectrometer on the computer (the QC sample is the same sample). After the mass spectrometry was completed, the peak map of each QC sample was analyzed to determine whether there was a deviation in the instrument performance during the mass spectrometry measurements. The primary and secondary mass spectra obtained by the mass spectrometer were then compared with the database. The mass spectrometry secondary fragmentation data were matched with the in-house metabolite standard secondary library and scored, metabolites with a similarity >80% were extracted and the metabolites were further identified, differentially analyzed and functionally annotated.

Data processing

Identification of metabolites

Using biological information to analyze the off-machine data of the mass spectrometer, XCMS software was mainly used for substance detection and metaX software was used to screen the detected substances quantitatively and differentially. Quantitative and differential metabolite screening was performed using metabolite primary m/z and

Table 1: Chromatographic and mass spectrometry conditions.

Time	Mobile phase composition
0~0.5 min	5% B
0.5~7 min	5%~100% B
7~8 min	100% B
8~8.1 min	100%~5% B
8.1~10 min	5% B

secondary fragment ions and databases. The first-level identification results were determined by matching with databases such as KEGG, the second-level spectra of the substances were compared with the in-house database and KEGG annotation was performed.

Quantitative analysis of metabolites

Quantitative metabolite information was obtained from the primary chromatographic area of the substance. The intensity information of each substance in each sample was extracted by XCMS and then the extracted data were subjected to quality control using metaX software, first removing low-quality peaks (more than 50% missing in QC samples or more than 80% missing in actual samples) in the ion removal. Then, the KNN method was used to fill in missing values, the PQN and QC-RSC methods were used for correction and the corrected data were filtered. That is, ions with a coefficient of variation (CV) >30% in all QC samples were filtered out.

Screening of differential metabolites

Metabolomics results were analyzed using the open-source software metaX and variable and multivariate analyses were performed to obtain differential metabolites between groups, including differential expression fold analysis, principal component analysis and partial least squares discriminant analysis (PLSDA). Three conditions were met at the same time: 1) the ratio of the material difference was greater than or equal to 2 or the ratio was less than ½; 2) the p value was less than 0.05; and 3) the VIP of the variable projection of the PLS-DA model was greater than or equal to 1.

RESULTS AND DISCUSSION

Results of metabolomic analysis of metabolites

Among all the detected metabolite species, there were 629 secondary metabolites that matched both the database m/z and database fragment ions and 287 different metabolites were detected in the model group compared with the normal group. Compared with the model group, 107 different metabolites were detected in the stem cell treatment group and 57 metabolites were found to be covaried.

Data quality control

1): Each color represents a sample and the peak shape trends of all samples were consistent, indicating the stability of the metabolome data instrument and the accuracy of metabolite identification (Fig 1).

2): The detection ranges of all metabolized ions were within 0-10 min, the retention times were within 0-10 min and the m/z mass-to-nucleus ratios of metabolite ions were within 0-1000. We found that metabolite ions peaked at approximately 4 min and the molecular weights of metabolite ions were approximately 400 (Fig 2).

3): A total of 629 metabolites were accurately identified in this experiment. The overall metabolites and their associated metabolic pathways are shown in the figure below (Fig 3).

4): For the biological replicates of the overall sample, A, B and C (6 biological replicates of each sample were essentially clustered together) are shown below (Fig 4).

5: We found that 287 metabolites were differentially expressed in the model and normal groups (Fig 5).

6): We found that 107 metabolites were differentially expressed in the stem cell treatment and model groups (Fig 6).

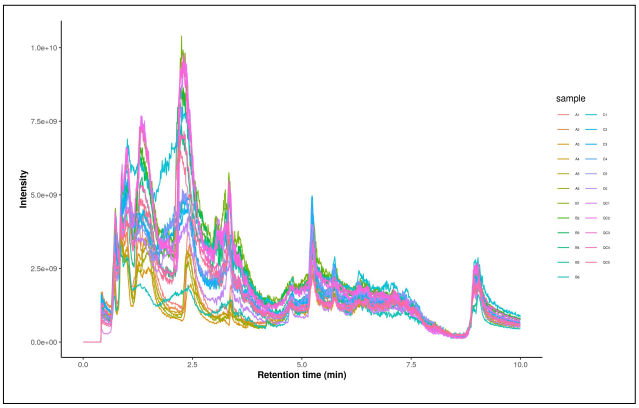

Fig 1: Ion chromatogram of TIC.

Each color represents a sample and the peak shape trends of all samples were consistent, indicating the stability of the metabolome data instrument and the accuracy of metabolite identification.

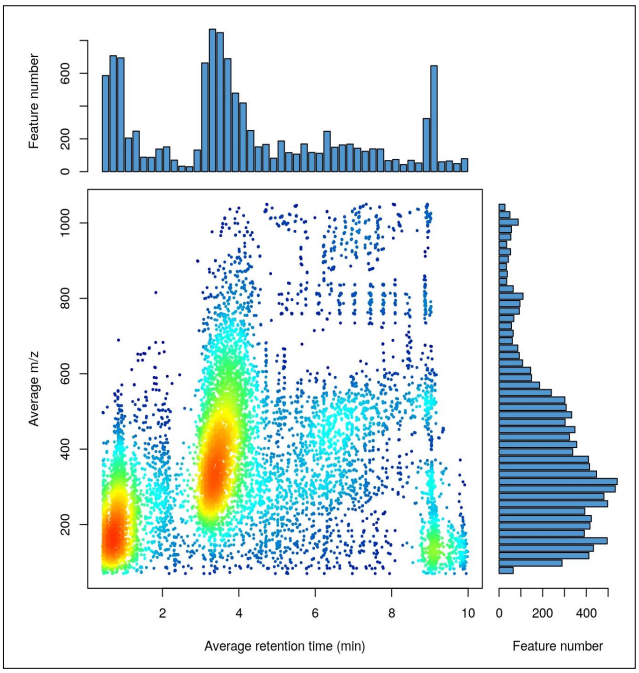

Fig 2: MZ-RT overall metabolic ion identification.

The detection ranges of all metabolized ions were within 0-10 min, the retention times were within 0-10 min and the m/z mass-to-nucleus ratios of metabolite ions were within 0-1000. We found that metabolite ions peaked at approximately 4 min and the molecular weights of metabolite ions were approximately 400.

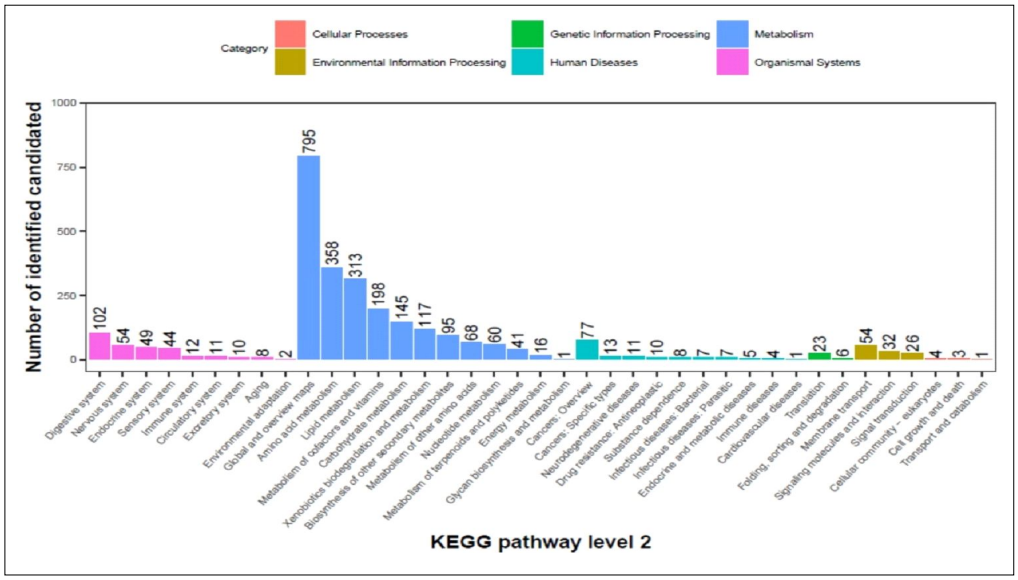

Fig 3: Overall metabolites and their associated metabolic pathways.
A total of 629 metabolites were accurately identified in this experiment. The overall metabolites and their associated metabolic pathways are shown in the figure.

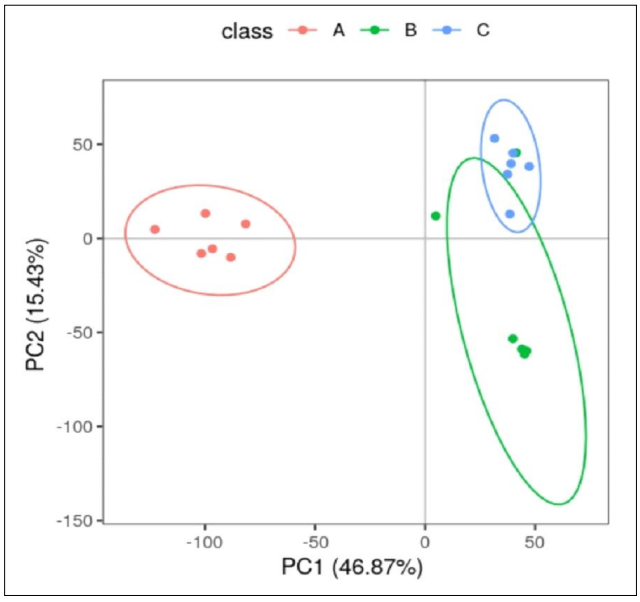

Fig 4: PCA diagram or the biological replicates of the overall sample, A, B and C (6 biological replicates of each sample were essentially clustered together).

Analysis of the differential metabolites in metabolic pathways

We found that there were 57 differential metabolites in common between the two comparison groups. These common differential metabolites are pathways that are highly related to stem cell treatment recovery. Through enrichment analysis, we found that á-linolenic acid and linoleic acid metabolism were the most significantly enriched pathways related not only to the above pathway-related stem cell treatment but also to lactate synthesis, sphingolipid metabolism and other pathways.

1): The differential metabolites of the normal and model groups intersected with those of the stem cell treatment and model groups (Fig 7 Venn diagram of differentially expressed metabolites) and 57 different metabolites are displayed in a heatmap (Fig 8 Common differentially expressed metabolites).

2): Pathway enrichment analysis for the 57 differential metabolites (Fig 9).

Trend analysis of common differential metabolites

Finally, we performed trend analysis on 57 metabolites (bioinformatics analysis was performed using the Omic Studio tools at https://www.omstudio.cn/tool) and identified 25 differential metabolites in the normal, model and stem cell treatment groups. Among the 25 metabolites, alpha-linolenic acid, linoleic acid, arachidonic acid and others can effectively resist inflammation and their increase after stem cell treatment indicates that inflammation was relieved. Eleven metabolites showed a trend of first increasing and then decreasing. The arginine and alanine levels of 11 metabolites increased in the model group, indicating that the model group had inflammatory changes and the inflammatory response was relieved after treatment, which is in line with stem cell therapy. The recovery of the curative effect of the model group indicates the metabolites upon which our research group will focus in later studies (Fig 10).

In modern local wars, various explosive weapons have high explosive power and large amounts of shrapnel can be projected in fan shapes or in three dimensions, with large killing areas and accurate attack targets [Li *et al*., 2018].

The killing effects of modern weapons have the characteristics of high speed, high efficiency, high intensity and soft kill (three high and one soft). These characteristics can cause serious injury consequences, mainly in the form of more serious injuries, multiple injuries and multiple burns. They are also associated with many psychological disorders and physiological imbalances, resulting in a high attrition rate, a high shock rate and a high operation rate (four more and three high), complicating modern war injuries and bringing greater difficulty to rescues (Hadziahmetovic, 1995; Klausner and Rozin, 1995). Among all kinds of war wounds, firearm injuries caused by high-speed and small-mass weapons represent the highest proportion of war wounds in modern local wars. The wounds are complex and the associated infections can be serious (Patzkowski *et al*., 2012; Yee *et al*., 2017). In research on injury caused to important organs, it was found that after the injury of the maxillofacial region with high-speed steel balls, the heart, lungs and other important organs of the animals exhibited small-scale flaky hemorrhages, which become the condition

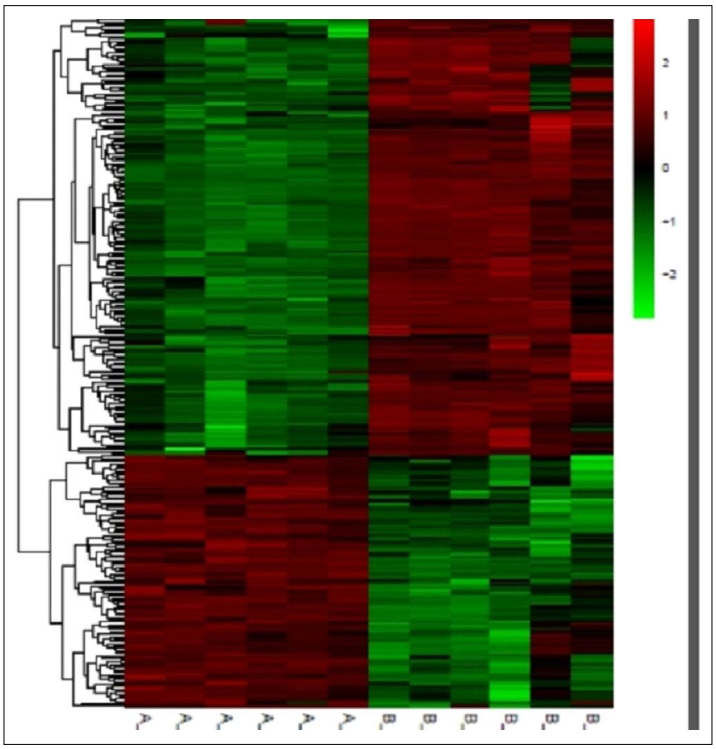

Fig 5: Heatmap of the differences between the model and normal groups.
We found that 287 metabolites were differentially expressed in the model and normal groups.

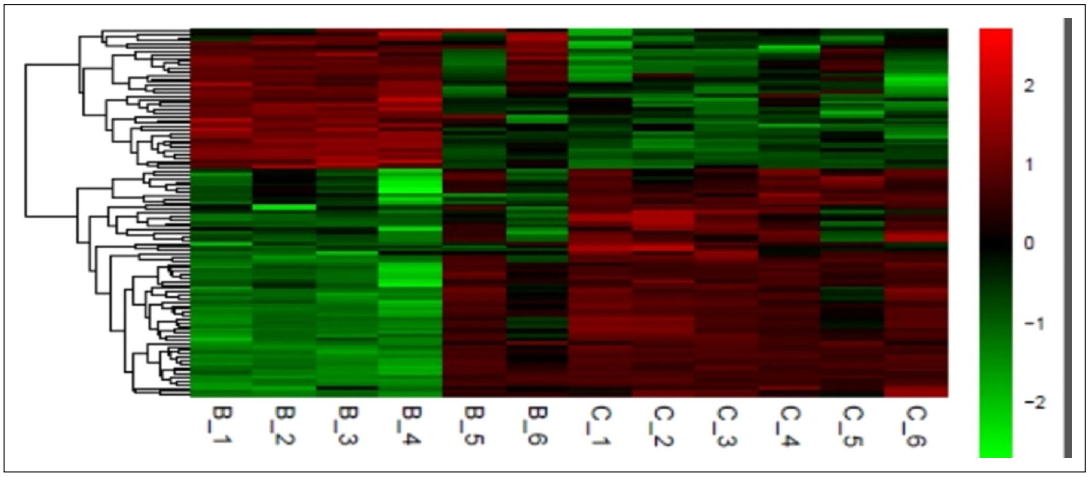

Fig 6: Heatmap of the differences between the treatment and model groups.
We found that 107 metabolites were differentially expressed in the stem cell treatment and model groups.

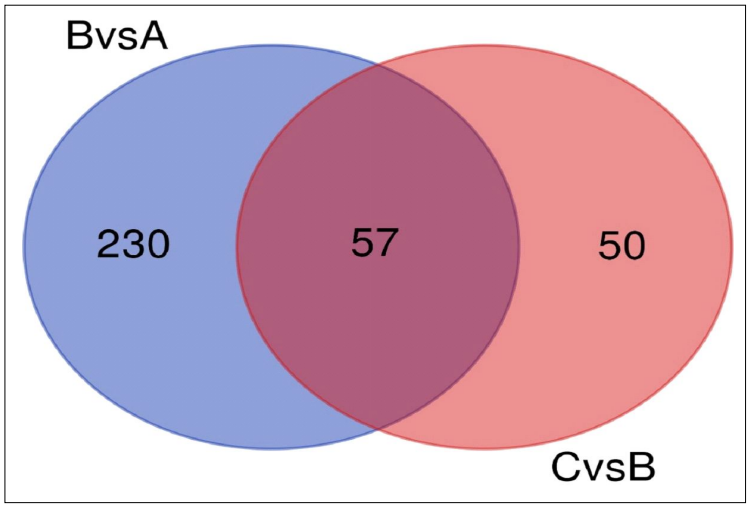

Fig 7: Venn diagram of differentially expressed metabolites.
The differential metabolites of the normal and model groups intersected with those of the stem cell treatment and model groups.

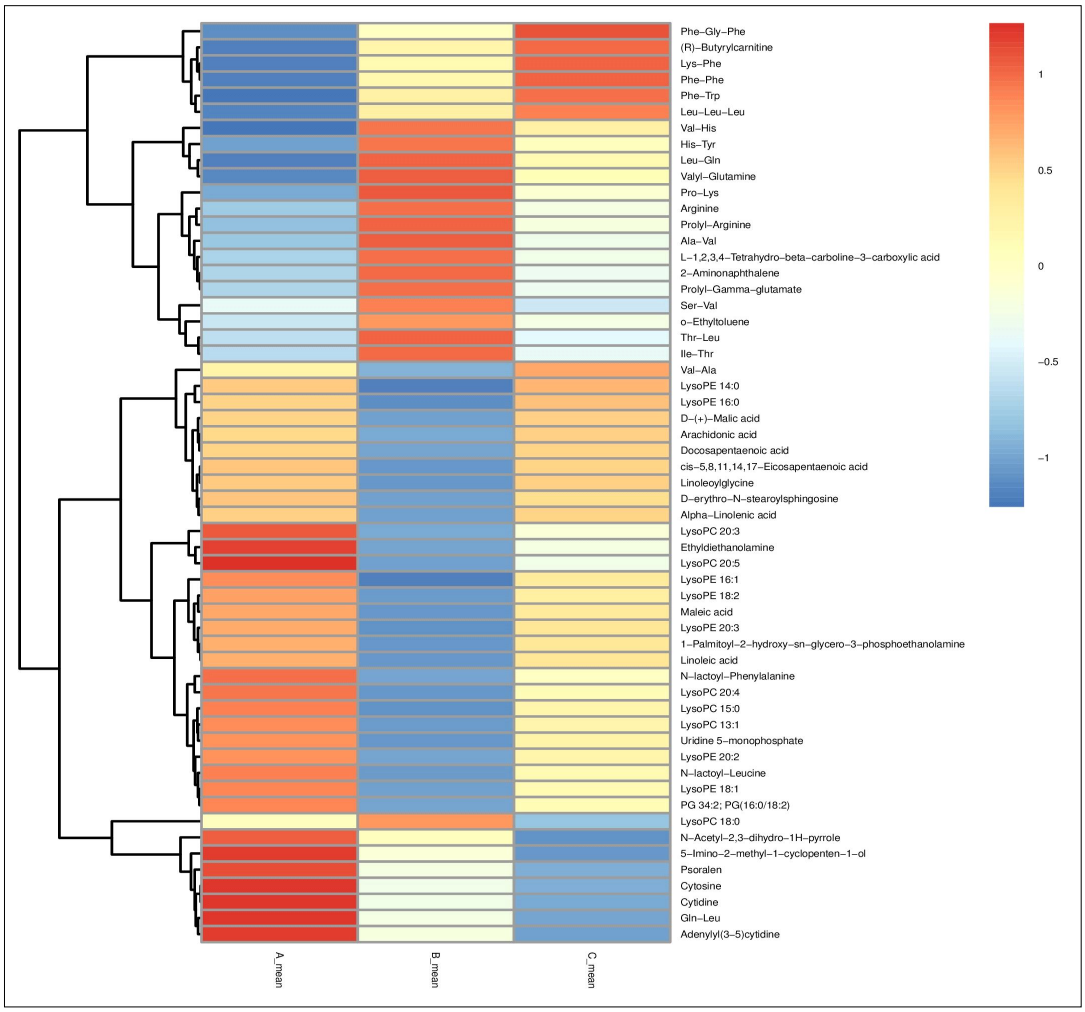

Fig 8: Common differentially expressed metabolites.
57 different metabolites are displayed in a heatmap.

and pathological basis for the occurrence and development of serious complications, such as acute respiratory distress syndrome, disseminated intravascular coagulation or multiple organ failure (Lyons, 2010;Del Sorbo and Slutsky, 2011; Lee *et al*., 2011;Huang *et al*., 2013). This series of posttraumatic syndromes is an important reason for the high mortality rate among troops. Rapid and effective control and treatment of posttraumatic syndrome is a hot research topic both at home and abroad. Therefore, it is of great military and scientific significance to establish a reproducible animal model for war-traumatic infection, systemic inflammatory response syndrome, shock and multiple organ failure and a new treatment method based on the animal model. The use of the tree shrew to establish a systemic inflammatory response syndrome model has the following advantages: the tree shrew is a nonhuman primate surrogate animal with abundant resources, low cost and a close relationship with humans. In recent years, this issue has received increasing attention, though the systemic inflammatory response syndrome model of tree shrews has been rarely reported at home and abroad.

We established a tree shrew systemic inflammatory response syndrome model and treated it with umbilical cord mesenchymal stem cells. Previous studies have shown that the model was successfully established and that the treatment effect was obvious. In this paper, we established control, treatment and model groups. Metabolomics analysis of the specimens showed that 25 differential metabolites in the normal, model and stem cell treatment groups showed trends of first decreasing and then increasing, while 11

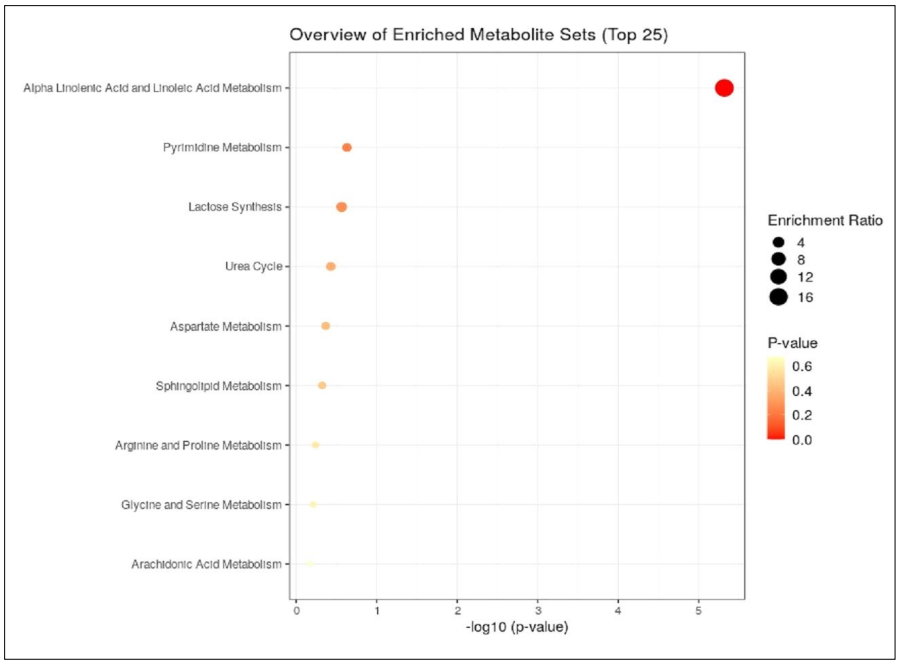

Fig 9: Pathway enrichment analysis.
Pathway enrichment analysis for the 57 differential metabolites.

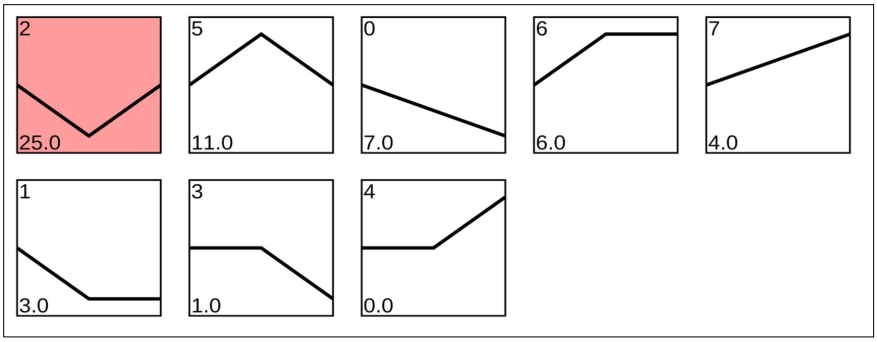

Fig 10: Trend analysis of metabolites.
Eleven metabolites showed a trend of first increasing and then decreasing. The arginine and alanine levels of 11 metabolites increased in the model group, indicating that the model group had inflammatory changes and the inflammatory response was relieved after treatment.

metabolites showed trends of first increasing and then decreasing. These findings are consistent with the recovery of the efficacy of the stem cell therapy model group and represent changes in inflammatory factors, indicating that the model group has a significant inflammatory response and that treatment with umbilical cord mesenchymal stem cells has the effect of reducing inflammatory factors, further proving the anti-inflammatory effect of umbilical cord mesenchymal stem cells. From the positive ion mode KEGG analysis results of the model group vs. the normal group, it can be seen that the inflammatory mediator regulation of the TRP channel pathway is meaningful; this pathway is the inflammatory mediator regulation of TRP channels, in line with our animal model of traumatic systemic inflammatory response syndrome.

CONCLUSION

These results all show that tree shrew umbilical cord mesenchymal stem cells are effective in the treatment of systemic inflammatory response syndrome. The experimental results of tree shrews have laid a solid foundation for the treatment of human beings. In the future, in-depth research will be needed before using this treatment in modern military medicine.

ACKNOWLEDEGMENT

We thank American Journal Experts for assisting with the English preparation of this manuscript.

Author contributions

Guang-Ping Ruan and Xiang Yao, made substantial contributions to the study conception and design, data acquisition and data analysis and interpretation.
Guang-Ping Ruan, Kai Wang and Xiang Yao conducted the experiments.

Xiang Yao and Shu-Qian Lin agree to be accountable for all aspects of the work and ensure that questions related to the accuracy or integrity of any part of the study will be appropriately investigated and resolved.

Xing-Hua Pan and Guang-Ping Ruan provided final approval of this version of the manuscript for publication.

Guang-Ping Ruan, Xing-Hua Pan, Shu-Qian Lin and Rong-Qing Pang were involved in drafting the manuscript or revising it critically for important intellectual content. All authors read and approved the final manuscript.

Funding Statement

This work was supported by grants from the Yunnan Science and Technology Plan Project Major Science and Technology Project (2018ZF007), the Yunnan Province Applied Basic Research Program Key Project (202101AS070039), the 920th Hospital of the PLA Joint Logistics Support Force In-hospital Technology Plan (2019YGB17, 2020YGD12) and the whole army experimental animal special (SYDW-020160004).

Conflict of interests

The authors declare that they have no competing interests.

REFERENCES

Anderson, S.L., Singh, B. (2017). Neutrophil apoptosis is delayed in an equine model of colitis: Implications for the development of systemic inflammatory response syndrome. Equine Vet J. 49(3): 383-88.

Del Sorbo, L., Slutsky, A.S. (2011). Acute respiratory distress syndrome and multiple organ failure. Curr Opin Crit Care. 17(1): 1-6.

Fang, S., Xu, C., Zhang, Y., Xue, C., Yang, C., Bi, H. *et al.* (2016). Umbilical cord-derived mesenchymal stem cell-derived exosomal microrna suppress myofibroblast differentiation by inhibiting the transforming growth factor-beta/smad2 pathway during wound healing. Stem Cells Transl Med. 5(10): 1425-39.

Garcia-Lamberechts, E.J., Martin-Sanchez, F.J., Julian-Jimenez, A., Llopis, F,. Martinez-Ortiz, D.Z.M., Arranz-Nieto, M.J. *et al.* (2018). Infection and systemic inflammatory response syndrome in older patients in the emergency department: A 30-day risk model. Emergencias. Ago; 30(4): 241-46.

Hadziahmetovic, Z. (1995). [The effect of organization of treatment of injuries on the occurrence of late complications of fractures caused by gunshots and explosions in war]. Med Arh. 49(3-4): 83-6.

Huang, P.M., Lin, T.H., Tsai, P.R., Ko, W.J. (2013). Intrapleural steroid instillation for multiple organ failure with acute respiratory distress syndrome. Shock. 40(5): 392-7.

Klausner, J.M., Rozin, R.R. (1995). Late abdominal complications in war wounded. J. Trauma. 38(2): 313-7.

Lee, B.J., Chen, C.Y., Hu, S.Y., Tsan, Y.T., Lin, T.C., Wang, L.M. (2011). Otalgia and eschar in the external auditory canal in scrub typhus complicated by acute respiratory distress syndrome and multiple organ failure. BMC Infect Dis. 30: 11:79.

Li, T., Sun, X.Z., Lai, D.H., Li, X., He, Y.Z. (2018). Fever and systemic inflammatory response syndrome after retrograde intrarenal surgery: Risk factors and predictive model. Kaohsiung J. Med Sci. 34(7): 400-08.

Lyons, W.S. (2010). Fresh frozen plasma is not independently associated with a higher risk of multiple organ failure and acute respiratory distress syndrome. J. Trauma. 68(3): 749. doi: 10.1097/TA.0b013e3181c9c4d2.

Mahassadi, A.K., Nguieguia, J.L.K., Kissi, H.Y., Awuah, A.A., Bangoura, A.D., Doffou, S.A. *et al.* (2018). Systemic inflammatory response syndrome and model for end-stage liver disease score accurately predict the in-hospital mortality of black African patients with decompensated cirrhosis at initial hospitalization: A retrospective cohort study. Clin Exp Gastroenterol. 11: 143-52.

Patzkowski, J.C., Blair, J.A., Schoenfeld, A.J., Lehman, R.A., Hsu, J.R. (2012). Multiple associated injuries are common with spine fractures during war. Spine J. 12(9): 791-7. (2016). https://doi.org/10.1186/s13287-016-0385-1.

Ruan, G.P., Yao, X., Liu, J.F., He, J., Li, Z.A., Yang, J.Y. *et al*. (2016). Establishing a tree shrew model of systemic lupus erythematosus and cell transplantation treatment. Stem Cell Res Ther. 7(1): 121.

Ruan, G.P., Yao, X., Mo, P., Wang, K., Yang, Z.L., Tian, N.N. *et al*. (2021). Establishment of a systemic inflammatory response syndrome model and evaluation of the efficacy of umbilical cord mesenchymal stem cell transplantation. Cells Tissues Organs. 210(2): 118-34.

Wagner, R., Piler, P., Uchytil, B., Halouzka, R., Kovaru, H., Bobkova, M. *et al*. (2016). Systemic inflammatory response syndrome is reduced by preoperative plasma-thrombo-leukocyte aphaeresis in a pig model of cardiopulmonary bypass. Biomed Pap Med Fac Univ Palacky Olomouc Czech Repub. 160(3): 399-406.

Ward, L., Paul, M. andreassen, S. (2017). Automatic learning of mortality in a CPN model of the systemic inflammatory response syndrome. Math Biosci. 284: 12-20.

Xu, R. (2019). Combination of systemic inflammatory response syndrome and Quick-SOFA: Is This a new vital model to initiate or escalate therapy in patients with sepsis? Chest. 155(1): 243-44.

Yee, M.K., Janulewicz, P.A., Seichepine, D.R., Sullivan, K.A., Proctor, S.P., Krengel, M.H. (2017). Multiple mild traumatic brain injuries are associated with increased rates of health symptoms and gulf war illness in a cohort of 1990-1991 gulf war veterans. Brain Sci. 7(7). 79. doi: 10.3390/ brainsci7070079.